Original Article

Institution of MECHANICAL ENGINEERS
Journal of ENGINEERING TRIBOLOGY

Proc IMechE Part J:
J Engineering Tribology
226(5) 343–349

DOI: 10.1177/1350650111432998
pij.sagepub.com
SAGE

Grid generation in hydrodynamic and elastohydrodynamic lubrication using algebraic multigrid method

MP Noutary[1], CH Venner[2] and AA Lubrecht[1]

Abstract

This article analyses the generation of 'optimal' grids for lubrication problems including hydrodynamic and elastohydrodynamic lubrication. It does this by using existing numerical solutions on (very) fine and regular grids, and studying the coarse grids generated by algebraic multigrid. This article analyses two hydrodynamic lubrication applications, the circular hydrodynamic lubrication contact and the rough surface lubrication. The latter subject is currently attracting a large interest from both industry and university. A third elastohydrodynamic lubrication application highlights the strong coupling in the high-pressure zone.

Keywords

Hydrodynamic lubrication, elastohydrodynamic lubrication, liner roughness, optimum grid solution

Date received: 3 October 2011; accepted: 23 November 2011

Introduction

The numerical solution of lubrication problems involves the solution of the Reynolds equation, which at first sight is a simple elliptic partial differential equation (PDE) for the pressure when the gap height is given. However, when the gap height depends on the pressure terms, the coefficients in the equation may vary many orders of magnitude over the domain. For the case of surface roughness patterns or striations, the problem may exhibit strong anisotropy and/or discontinuous behaviour. For liquid lubricants, the cavitation condition introduces a non-linearity in the system. Under elastohydrodynamic lubrication conditions (EHL), the pressure will be so large that elastic deformation occurs with an order of magnitude similar to the characteristic length scale of the pressurised region, which is much larger than the gap height itself. The fluid flow and gap height have to be simultaneously solved from the Reynolds equation coupled with an elastic deformation calculation. In this case, the non-linearity is even stronger. Also, the character of the Reynolds equation changes. In the low-pressure region, it is an elliptic PDE for the pressure. In the high-pressure regions where the coefficients of the pressure terms are small due to the small film thickness and large deformation, it is an hyperbolic equation dictating the gap height with the pressure determined by the elasticity. The non-linearity and local changes of character are even more pronounced when the viscosity pressure dependence is taken into account. All these aspects were treated for the first time in the pioneering papers by Dowson et al.[1,2]

In retrospect, it is not surprising that it has taken quite some time before EHL problems could be efficiently solved and many papers in the literature deal with different aspects of solving the problem. Todays computers have become very fast and hence EHL solutions can be quickly obtained, even when using standard slowly converging iterative techniques. But these solutions are limited to one-dimensional steady-state problems (infinite line contact and smooth surface). However, the accurate solution of two-dimensional rough surface (transient) problems requires repeated solutions (every time step) and dense grids. Hence,

[1]Université de Lyon, INSA-Lyon, LAMCOS, France
[2]University of Twente, CWT, The Netherlands

Corresponding author:
AA Lubrecht, Universite de Lyon, INSA-Lyon, LAMCOS, CNRS-UMR 5259, Villeurbanne F69621, France.
Email: Ton.Lubrecht@insa-lyon.fr

grid efficiency and solver efficiency are absolute prerequisites for such cases.

The grid choice and its influence on computing time and solution precision are explicited in the study of Kudish and Coriteh.[3] However, it also influences the solution precision of black box FEM-type-based solvers, but this is rarely analysed.

The approach taken in this article is the use of a uniform (finest) grid, and hence a quest for solver efficiency.

MultiGrid (MG) methods have accelerated the solution of many large-scale problems since their conception in the late 1970s.[4] This basic formulation and implementation, referred to as *geometric* multigrid (GMG) has been applied to the lubrication problem since the mid-1980s.[5] The problems treated successfully range from hydrodynamic lubrication (HL) to EHL. Even though the gain in computing time is impressive, several problems had to be solved before the optimum convergence speed was obtained. These are common problems encountered when applying GMG to systems of equations and/or an equation with varying coefficients. The reason is that in these algorithms the coarsening is fixed. As an alternative Algebraic MultiGrid (AMG) was introduced, which, given a matrix-vector equation, by analysis of the equation coefficients automatically constructs a coarse grid according to the dependencies in the equations. In this article, aspects of AMG[6] are used to illustrate the fundamental dependencies in some lubrication problems and the resulting grid structure to be chosen.

This article is not meant to introduce AMG as an alternative numerical solution method to GMG algorithms already developed. When GMG works, it often is much faster as the differential and intergrid operators are dictated by the fixed coarsening, whereas in AMG they have to be computed in a set-up stage of the algorithm. However, assuming one starts of with the same uniform grid, the choices made in coarsening by AMG are an excellent way to illustrate the fundamental dependencies in the equations and problems considered when using standard MG. Therefore, these results may help guide coarsening in geometric MG and improve solver robustness for extreme cases. In this article, some AMG coarsening results are presented for lubrication problems. First for two HL applications, the circular HL contact,and the lubrication of a rough surface. The latter topic, transient lubrication of the rough cylinder liner, piston ring contact, is currently attracting a lot of interest. The precise numerical solution of this contact requires very fine grids and many timesteps. As such standard numerical methods result in unrealistically long computing times. Advanced numerical techniques, like MultiLevel techniques, require additional effort to develop adequate transfer operators and coarse grid operators. Finally, results for EHL are presented to illustrate the strong coupling in the high-pressure zone and the related inlet dominated film thickness behaviour. These results in fact confirm the choices made in the GMG solver development for these problems explained in the study of Venner and Lubrecht.[7]

Lubrication theory

The dimensionless two-dimensional (2D) Reynolds equation for the transient case read

$$\frac{\partial}{\partial X}\left(\epsilon\frac{\partial P}{\partial X}\right)+\frac{\partial}{\partial Y}\left(\epsilon\frac{\partial P}{\partial Y}\right)-\frac{\partial(\bar{\rho}H)}{\partial X}-\frac{\partial(\bar{\rho}H)}{\partial T}=0 \qquad (1)$$

The boundary conditions are $P(X_a,\ Y,\ T)=P(X_b,\ Y,\ T)=P(X,\ Y_a,\ T)=P(X,\ Y_b,\ T)=0,\ \forall T$, where X_a, X_b, Y_a and Y_b denote the boundaries of the domain. Furthermore, the cavitation condition $P(X,\ Y,\ T)\geq 0$, $\forall X,\ Y,\ T$ must be satisfied. ϵ and $\bar{\lambda}$ are defined according to

$$\epsilon=\frac{\bar{\rho}H^3}{\bar{\eta}\bar{\lambda}} \qquad \bar{\lambda}=\frac{12\eta_0 u_m R_x^2}{b^3 p_h}$$

For the HL problem, the density $\bar{\rho}$ and viscosity $\bar{\eta}$ are assumed constant. For the EHL case, the density $\bar{\rho}$ is assumed to depend on the pressure according to the Dowson and Higginson relation and the Roelands viscosity pressure relation is used. This means that for large values of the pressure, the viscosity goes (almost) exponentially to infinity.

The film thickness equation is made dimensionless using the same Hertzian parameters. For the HL case, the deformation term is zero

$$H(X,Y,T)=H_0(T)+\frac{X^2}{2}+\frac{Y^2}{2}+\frac{2}{\pi^2}\int_\Omega\frac{P(X',Y',T)\,\mathrm{d}X'\,\mathrm{d}Y'}{\sqrt{(X-X')^2+(Y-Y')^2}} \qquad (2)$$

where $H_0(T)$ is an integration constant.

At all times, the force balance condition is imposed, i.e. the integral over the pressure must balance the externally applied contact load. This condition determines the value of the integration constant $H_0(T)$ in equation (2). Expressed in the dimensionless variables it reads

$$\int_\Omega P(X,Y,T)\,\mathrm{d}X\,\mathrm{d}Y-\frac{2\pi}{3}=0,\quad \forall T \qquad (3)$$

In physical terms, this equation means that the acceleration forces of the contacting bodies are neglected.

Algebraic multigrid

To enable a numerical solution, the continuous problem, e.g. equations (1) to (3), are discretised on a grid. Consider equation (1) and assume H given as in HL applications. The discretisation at each time(step) results in an equation for each index i associated with a location at the grid

$$\sum_j a_{ij}u_j = f_j \tag{4}$$

for $0 \leqslant i \leqslant n$ which in matrix-vector can be written as

$$A\mathbf{u} = \mathbf{f} \tag{5}$$

where A is the matrix with each row containing equations (4), $\mathbf{u}$ the vector with all unknown e.g. the pressure values, and $\mathbf{f}$ the right-hand side vector with all known terms such as the wedge term in the rigid surface case. The system can be solved directly or iteratively (Jacobi relaxation, Gauss Seidel relaxation, Conjugate Gradient, etc). In both cases, the computing time often increases quadratically or worse with the number of nodes. For iterative methods, this is due to the slow asymptotic error reduction. The principle of Multigrid techniques is to accelerate convergence by finding an accurate approximation for the slow to converge error components. The slow error components are solved using a coarser scale problem containing less unknowns using the result to correct the original problem. The most widely applied implementation is GMG. In PDE problems, slow to converge errors are often physically smooth components and the coarser scale is chosen to be a grid with twice the mesh size in each direction. MG algorithms have the prospect of solving a problem using a computational effort proportional to the number of unknowns. For a detailed description, and applications to HL and EHL lubrication problems, the reader is referred to.[7–10] As the coarsening is fixed in GMG, it is crucial to *choose* or *develop* an iterative scheme such that indeed a geometrically smooth error in all directions is left behind on the grid. An alternative approach, AMG was developed for general cases not necessarily related to PDE problems and/or when the slow to converge errors are not a priori known.[6,11] In this case, a simple iterative process is chosen and the coarsen is tailored such that the reduced set of equations and unknowns yields an accurate approximation of exactly those components the iterative scheme could not reduce. Applied to, e.g. scalar elliptic PDEs AMG is often more robust and better applicable in a black box setting than GMG. However, it is also computationally more expensive due to the set-up of the tailored coarsening. Also, accounting for non-linearity is more complicated than for GMG. Therefore, AMG only pays off for the more difficult problems. An intermediate approach, for those problems hard to solve with standard GMG, is to develop 'advanced' coarsening strategies. These may be obviously derived from analysis of the equations. However, when coefficients vary strongly, AMG tools may be helpful to identify specific coarsening strategies. For some lubrication problems the coarsening suggested by AMG is illustrated in this article. Below a brief introduction of AMG is given. A more detailed introduction is given in the study of Briggs et al.[10] Advanced reading can be found in the study of Ruge and Stüben[6] and Trottenberg et al.[8] A current trend in multigrid algorithm development is a generalisation of AMG, referred to as Bootstrap AMG.[12–14]

Assume a simple local iterative algorithm is used obtain the solution of equation (5), starting with some first approximation $\mathbf{u}_0$. Let $\tilde{\mathbf{u}}$ be the current approximation after some iterations and $\mathbf{r}$ denote the vector of *residuals* defined as

$$\mathbf{r} = f - A\tilde{\mathbf{u}} \tag{6}$$

The residual is a direct measure of the error $e_i = u_i - \tilde{u_i}$. This is most obvious for a linear operator

$$\mathbf{r} = A\mathbf{u} - A\tilde{\mathbf{u}} = A\mathbf{e} \tag{7}$$

Components that are slow to converge in iterative processes are the components for which $r \approx 0$, whereas e is not small, so, considering the i^{th} equation of the system. For such errors

$$\sum_j a_{ij}e_j \approx 0 \rightarrow a_{ii}e_i \approx -\sum_{j \neq i} a_{ij}e_j \tag{8}$$

Hence, for slow-to-converge errors, the value in point i is the weighted average of its values in the points j which appear in the i^{th} equation with the weights being the relative value of their coefficients to the central coefficient a_{ij}/a_{ii}. The larger its value, the more strongly dependent the value of the error in point i is on the value in the point j. Let U denote the set of datapoints i for $0 \leq i \leq n$. The concept in AMG is now to use the strong and weak dependencies in the matrix to select a subset of the datapoints denoted by C which can provide an accurate representation of the (remaining) error not reduced by the relaxation and from which the value of this error in the other points, denoted by F can be obtained by a suitable interpolation. Of course $C \cup F = U$. The process of C and F splitting is also referred to as *coloring*.[10] An unknown i is defined to strongly depend on an unknown j that appears in the equation for unknown i when

$$a_{ij} \geq \theta \max_{j \neq i}(a_{ij}) \tag{9}$$

where θ is some threshold, typically $\theta = 0.1$. During the coloring, the number of points j that strongly depend on a point i is counted. This dependency count is used as a measure for its potential as a C point. More details on the coloring process can be found in the study of Briggs et al.[10] The resulting C–F splitting reflects the nature of the slow to converge errors. This is illustrated in Figure 1 for the case of the anisotropic Poisson 2D equation

$$\frac{\partial^2 u}{\partial x^2} + \epsilon \frac{\partial^2 u}{\partial y^2} = f(x, y) \tag{10}$$

with appropriate boundary conditions. In Figure 1, the C–F splitting is presented for the case of the standard five-point discretisation of equation (10) on a uniform grid. First, for $\epsilon = 1$, all points influence each other with equal strength which leads to a uniform coarsening in a checkerboard manner. Next, when $\epsilon \ll 1$, the equations are much more strongly coupled in x direction than in y direction so the remaining error after relaxation is smooth in the x direction only and coarsening will be done in this direction. When $\epsilon \gg 1$, the situation is reversed and the coloring will yield a C–F splitting such that coarsening is done only in the y direction. For such cases GMG with fixed uniform coarsening in each direction requires special measures in the relaxation, i.e. line relaxation in the direction of strong coupling for efficiency, or indeed, the coarsening should only be done in one direction.[7] The advantage of AMG is that the coarsening will also automatically adapt locally when the behaviour is different in different parts of the domain. This is illustrated by the third figure which shows the C–F splitting for the case $\epsilon = 0$ in the left half of the domain and $\epsilon = 1000$ in the right half.

Although this article focuses on the result of the C–F splitting, i.e. the suggested coarsening, for the sake of completeness the description of AMG is continued. The next step is to find an equation for the solution of the e values in the C nodes. First, an interpolation is defined. Given the value of e in all points $I \in C$, for any point i in F

$$e_i^F = \sum_{I \in S_i^C} \omega_{Ii} e_I^C \tag{11}$$

where S_i^C is a subset of the C points, referred to as the 'coarse interpolatory set', i.e. the set of C points involved in the interpolation to point i, and ω_{Ii} are the interpolation weights. In matrix notation, the interpolation can be written as

$$\mathbf{e} = II_C^U \mathbf{e}^C \tag{12}$$

where II_C^U is the matrix of interpolation. For each row coinciding with an F point, the entries are the interpolation weights ω_{Ii}. For each row coinciding with a C point, its entry is trivially unity at the column with the index of the C point and zero at all other positions in the row. The interpolation should be such that it is accurate for those components which are to be solved on the reduced set and were badly reduced by relaxation. Its construction is based on equation (8),

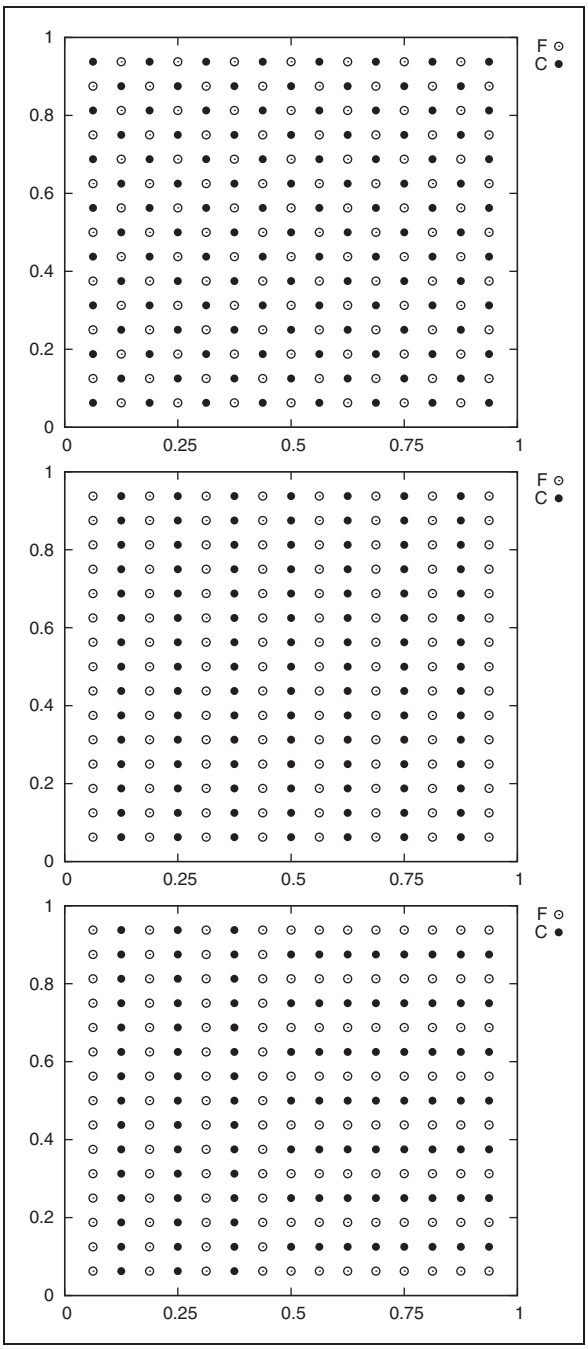

Figure 1. Examples of C and F splitting obtained for Poisson 2D equation (10) for $\epsilon = 1$ (isotropic), $\epsilon = 0$ (anisotropic, strong x coupling), and mixed ($\epsilon = 0$ for $x <= 0.5$ and $\epsilon = 1000$ for $x > 0.5$).

and the information of the strong and weak coupling in the matrix. The resulting interpolation weights are matrix entry dependent.[6,10] Having defined an interpolation, by definition its transpose operation defines a restriction which, in matrix notation, can be written as

$$\mathbf{e}^C = I I_U^C \mathbf{e} \tag{13}$$

Applying equation (13) to equation (6), using (12) now leads to the following reduced problem

$$A^C \mathbf{e}^C = r^C \tag{14}$$

where $A^C = I I_U^C A I I_C^U$, which is the equivalent of the Galerkin coarse grid operator in GMG, and $r^C = I I_U^C \mathbf{r}$.

Equation (14) can now be solved for $\mathbf{e}^C$, e.g. e in all C points. Subsequently, using (12) a new approximation $\mathbf{u}$ to $\mathbf{u}$ is obtained from

$$\mathbf{u} = \tilde{\mathbf{u}} + I I_C^U \mathbf{e}^C \tag{15}$$

This 'coarse grid' correction procedure can be recursively applied when the coarse problem is still too large to solve directly in a small amount of work. The general idea is the same as in GMG: Iterative solution on the system of equations is replaced by a recursive coarse grid correction cycling which accelerates convergence to a speed independent of the number of nodes.

The actual implementation of AMG is not trivial. In particular, one needs to take care to efficiently set up the datastructure for minimal storage, and carry out the coarsening, i.e. coloring, computation of coarse grid operator, and of interpolation and restriction in such a way that everything is done in an amount of work at most proportional to the number of unknowns. However, for the purpose of this article, the major point is to see what coarsening is suggested for the some characteristic lubrication problems.

HL: cavitation boundary

Figure 2 shows a coarse grid generated by the AMG algorithm. The finest grid is a uniform square grid extending from $X = -4.5$ to $X = 1.5$ and from $Y = -3.0$ to $Y = 3.0$. Note the discretisation at 45° in the inlet zone, and the complete absence of a mesh in the cavitation zone. Also note that the grid spacing is very similar in X and Y direction, indicating comparable derivatives in both directions. Hence, the standard square grid with identical mesh size in X and Y directions is a very good choice. As the cavitation frontier is initially unknown, this grid has to extend substantially into the diverging zone of the bearing ($X > 0$).

HL: rough surface lubrication

The transient lubrication of rough surfaces using measured surface roughness remains a formidable

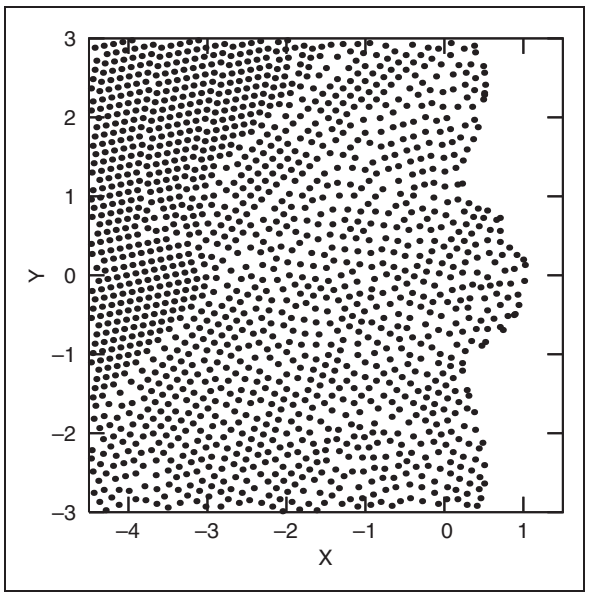

Figure 2. Coarse grid of circular HL problem.

computational challenge. This is especially true for the cylinder liner-piston ring contact, as the liner roughness is dominated by the (directional) cross-hatched pattern of grooves. Figure 3 shows a surface roughness measurement and a relatively coarse grid (coarsened three times) of the cylinder liner lubrication. The coarse grid clearly shows a cross-hatched pattern at roughly 60°, with lower point densities (lighter zone in the grid point figure) in the high slope areas (darker areas in the iso-height figure). The point density in the valleys and on the plateau's is high and roughly uniform. The lower density slopes indicate that the equations on the plateau's and in the valleys are relatively independent (decoupled).

This is a particular case of a problem with strongly discontinuous coefficients, as studied by Alcouffe et al.[15] and Dendy.[16] The general conclusion from this study was to avoid 'straddling' these discontinuities, both with the differential operator and the interpolation and restriction operators. In practice, this means that the solutions from the valleys and from the plateau's should not be mixed. Furthermore, it is clear that the flow in the valleys is very important, and should be correctly described on the coarse grids. This will most likely require multiple and rotated (aligned) coarse grids.

A word on the figure, and the choice of a rather dense grid, to illustrate the low density in the high slope regions. When using fewer points, the groove size to grid size makes the low density slopes more difficult to spot.

EHL: high-pressure zone

For the EHL case, a high-pressure zone exists in which the viscosity η goes exponentially to infinity. As a

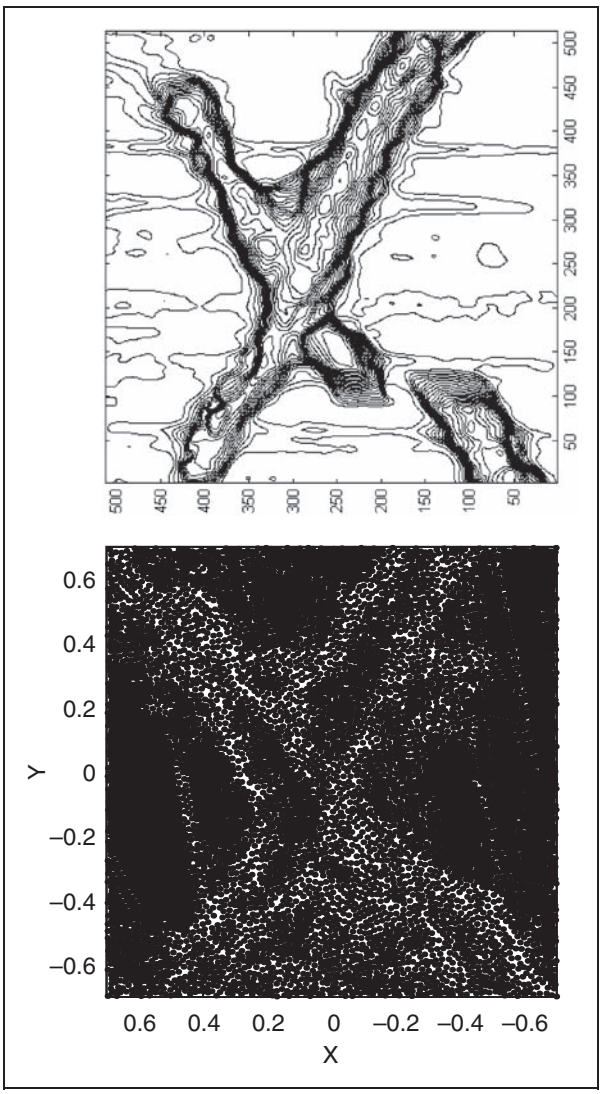

Figure 3. Cylinder-liner measured roughness and coarse grid of transient HL calculation.

result, the ϵ term goes exponentially to zero. This means that the first two terms of the Reynolds equation can be neglected with respect to the last two terms. As a consequence, the Reynolds equation in the high-pressure zone reduces to

$$\frac{\partial(\bar{\rho}H)}{\partial X} + \frac{\partial(\bar{\rho}H)}{\partial T} = 0 \tag{16}$$

In case of a stationary problem, and neglecting compressibility it follows that $H(X, Y) = C(Y)$, i.e. the film thickness in the high-pressure zone is constant in the X direction. This constant is determined by the inlet conditions. Numerically, this gives rise to a 'weak coupling' in the Y direction, and only line relaxation in the X direction delivers a good performance.

Figure 4 shows a coarse grid generated by the AMG algorithm for the EHL problem. The finest grid is a

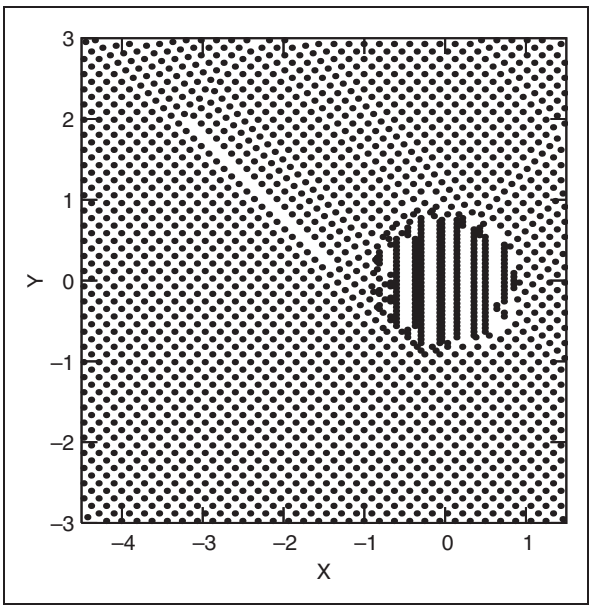

Figure 4. Coarse grid of circular EHL problem.

square grid extending from $X = -4.5$ to $X = 1.5$ and from $Y = -3.0$ to $Y = 3.0$. Note the discretisation at 45° in the (low pressure) inlet zone, as was observed in the HL problem. Also note that the grid spacing in the high pressure zone $X^2 + Y^2 < 1$ is non-uniform. The spacing in X direction is much larger than the spacing in Y direction. The weak coupling in the Y direction requires a line solver on a regular grid.[17] AMG solves this problem using semi-coarsening, i.e. the coarser grid has the same mesh size in Y direction as the finer grid. Coarsening only occurs in the X direction.

Conclusion

This study uses AMG coarse grid generator to study 'optimum' grid for the case of HL and EHL. These grids can inspire FEM grid or for MG coarse grid generation, as they highlight the strong coupling of the equations.

For the low-pressure HL and EHL zones, an optimal grid at 45° is generated. Hence, a standard regular grid is close to optimal. In the high-pressure EHL zone, semi-coarsening is applied, to deal with the weak coupling in Y direction. A semi-coarsened grid is close to optimal, whereas on a regular grid line-relaxation is required to obtain acceptable performance.

For the rough surface lubrication, AMG indicates that the pressure distribution on the plateau's and in the valleys are relatively independent. As such the coarse grid should mix as little as possible, the plateau and the valley solution (no averaging!). Work on the development of both transfer operators and multiple coarse grid operators is ongoing. Furthermore, the

authors are implementing an interpolation that is deactivated in the high slope zone, in order to avoid the averaging over different flow domains. A similar implementation applies to the cavitation boundaries.

Funding

This research received no specific grant from any funding agency in the public, commercial, or not-for-profit sectors.

Acknowledgements

The authors would like to thank Mr H. Bouassida for the pressure calculation of the rough cylinder liner piston ring contact and Dr P. Sainsot for the cylinder liner roughness measurement.

References

1. Dowson D and Higginson GR. *Elastohydrodynamic lubrication: the fundamentals of roller and gear lubrication*. Oxford, Great Britain: Pergamon Press, 1966.
2. Hamrock BJ and Dowson D. Isothermal elastohydrodynamic lubrication of point contacts, part I: Theoretical Formulation. *ASME J Lub Technol* 1976; 98: 223–229.
3. Kudish II and Covitch MJ. *Modeling and analytical methods in tribology*. Boca Raton, FL: Chapman and Hall/CRC press, 2010.
4. Brandt A. Multi-level adaptive solutions to boundary value problems. *Math Comp* 1977; 31: 333–390.
5. Lubrecht AA, ten Napel WE and Bosma R. Multigrid, an alternative method of solution for two-dimensional elastohydrodynamically lubricated point contact calculations. *ASME J Tribol* 1987; 109: 437–443.
6. Ruge J and Stüben K. Algebraic Multigrid (AMG). In: SF McCormick (ed.) In: *Multigrid methods*. Philadelphia: SIAM, Frontiers in Applied Mathematics, 1987, pp.169–212.
7. Venner CH and Lubrecht AA. *MultiLevel methods in lubrication*, vol. 37, USA, Elsevier: Tribology Series, 2000, p.379.
8. Trottenberg U, Oosterlee C and Schueller A. *Multigrid*. San Diego, USA: Academic Press, 2001.
9. Wesseling P. *An introduction to multigrid methods*. Flourtown, USA: R.T. Edwards, Inc, 2004.
10. Briggs WL, Emden Henson V and McCormick S. *A multigrid tutorial*, 2nd ed. US: SIAM, 2007.
11. Brandt A. Algebraic Multigrid Theory: The symmetric case. *Appl Math Comput* 1986; 19(1-4): 23–56.
12. Brandt A. General highly accurate algebraic coarsening. *Electronic Trans Numer Anal* 2000; 10: 120.
13. Falgout RD, Brannick J, Brezina M, et al. *J. Phys Conf Series* 2005; 16: 456–460.
14. Manteuffel T, McCormick S, Park M and Ruge J. Operator-based interpolation for bootstrap algebraic multigrid. *Numer Linear Algebra Appl* 2010; 17(2-3): 519–537.
15. Alcouffe RE, Brandt A, Dendy JE and Painter JW. The multigrid methods for the diffusion equation with strongly discontinuous coefficients. *SIAM J Sci Stat Comput* 1981; 2: 430–454.
16. Dendy JE. Black box multigrid for nonsymmetric problems. *Appl Math Comput* 1982; 13: 261–284.
17. Venner CH and ten Napel WE. Multilevel solution of the EHL circular contact problem, part 1: Theory and numerical algorithm. *Wear* 1992; 152: 351–367.

Appendix

Notation

a	coefficients of A (AMG)
A	matrix of influence coefficients (AMG)
b	radius of Hertzian contact $b = \sqrt[3]{(3FR_x)/(2E')}$
e	error (AMG)
E'	reduced modulus of elasticity $2/E' = (1-\nu_1^2)/E_1 + (1-\nu_2^2)/E_2$
f	right hand side (AMG)
F	external load
h	film thickness
H	dimensionless film thickness $H = hR_x/b^2$
n_x, n_y	number of (grid)points in x,y directions
p	pressure
p_h	maximum Hertzian pressure $p_h = (3F)/(2\pi b^2)$
P	dimensionless pressure $P = p/p_h$
R_x	reduced radius of curvature in x $1/R_x = 1/R_{1x} + 1/R_{2x}$
R_y	reduced radius of curvature in y, $R_y = R_x$
T	dimensionless time $T = tu_m/b$
u_m	mean velocity $u_m = (u_1 + u_2)/2$
u	solution (AMG)
$\tilde{u}$	approximate solution (AMG)
x	coordinate in direction of rolling
X, X'	dimensionless coordinate $X = x/b$
y	coordinate perpendicular to x
Y, Y'	dimensionless coordinate $Y = y/b$
α	pressure viscosity index
ϵ	coefficient in Reynolds' equation $\epsilon = (\bar{\rho}H^3)/(\bar{\eta}\bar{\lambda})$
Δ_T	dimensionless time step
Δ_X, Δ_Y	dimensionless mesh size in X, Y
$\bar{\eta}$	dimensionless density $\bar{\eta} = \eta/\eta_0$
ρ	density
$\bar{\rho}$	dimensionless density $\bar{\rho} = \rho/\rho_0$